Biomaterials and Tissue Technology

Research Article ISSN: 2398-970X

Porous poly (2-oxazoline) scaffolds for developing 3D primary human tissue culture

David J. van der Heide[1], Bart Verbraeken[3], Richard Hoogenboom[3], Tim R. Dargaville[2*] and Danica K. Hickey[1*]

[1]Biomedical Sciences, Chronic Disease and Ageing Program, Institute of Health & Biomedical Innovation, Queensland University of Technology, Australia

[2]Tissue Repair and Regeneration Program, Institute of Health and Biomedical Innovation, Queensland University of Technology, Australia

[3]Supramolecular Chemistry Group, Department of Organic Chemistry, Ghent University, Belgium

Abstract

The development of biologically inert synthetic scaffolds to support the 3D growth of human cells *in vitro* is essential in understanding the complex interactions between multiple cell types in tissue. A base 3D tissue culture scaffold without endocrine or growth factor interference from the substrate is key to providing a controllable biologically representative *in vitro* experimental model. Here we describe the cross-linking of a water soluble protein resistant polymer based on poly(2-alkyl-2-oxazoline) (PAOx), conjugated with cell binding peptides for use in human primary stromal cell 3D culture *in vitro*. Using a temperature controlled crystallization and freeze-dry process, the induction of a porous network structure within pre-cured hydrogels allows for the addition, attachment and growth of both mouse and human stromal cell lines within the scaffolds. We further show that scaffolds conjugated with the cell binding motif arginine-glycine-aspartic acid (RGD), support primary human cell attachment and growth. Morphological differences were observed by cells expanding across scaffold pores of the RGD conjugated scaffolds, while little adhesion was observed in scaffolds not containing RGD. The observed differences suggest a requirement for including RGD for PAOx-based 3D tissue culture scaffolding focusing on primary human stromal cells. PAOx scaffolds including RGD can therefore be used to generate 3D primary human stroma for use as a reproducible in vitro human model.

Introduction

Human epithelial tissues are composed of organised layers incorporating multiple cells types, such as stromal and epithelial cells, to form structural barriers between internal organ systems and the outside environment. These epithelial barriers constitute a major portal of entry for pathogenic organisms and are protected by a large co-ordinated mucosal immune system. Immunological responses require a coordinated interaction between these cells types through both physical interactions and secreted molecules within tissue to maintain homeostasis or protect against infection and disease [1]. Understanding these interactions is central to our ability to prevent infections or their pathological outcomes. Traditional 2-dimensional cell culture has proved to be a powerful tool in biomedical research, however, 3-dimensional (3D) models offer a more biologically representative system for the multicellular nature of cells *in vivo* [2]. Weaver *et al.* showed that a dysplastic monolayer cell line (HMT-3522) displayed reversion to normal cellular physiology when grown in 3D [3] which can be attributed to the alteration of gene expression [4]. Experimentally, explant tissues represent the most accurate 3D cellular model *in vitro* to date as they retain the complex multicellular structures of the *in vivo* tissue sampled [5,6]. However, small tissue sample volumes make explants impractical for wide scope investigations. To maintain the biological relevance seen in explant samples, numerous products and methods are available for growing cells in 3D scaffolds – the most commonly used systems contain a cocktail of carbohydrates, growth factors, hormones, and undefined proteins [7,8]. While this cocktail improves cell adhesion and growth, experiments involving steroid hormones and even drug interactions may be altered or masked by biological factors within these systems.

The ongoing development of polymer architectures provides a novel opportunity to provide scaffolds for 3D tissue culture that overcome inherent biological interactions observed with current systems [9]. Many synthetic hydrogel scaffolding systems have been developed using a range of polymer materials. The gold standard for biomedical applications, polyethylene glycol (PEG), exhibits low levels of biological interactions, and has been used to engineer a range of biological structures from bone-ligament interfaces [10] to extra cellular matrix (ECM) [9]. However, the structure of PEG restricts versatility as polymerization sites must be sacrificed if additional organic functional groups are required [1,12].

As an alternative to PEG hydrogels, poly(2-alkyl-2-oxazoline) (PAOx) has been explored to support biological *in vitro* 3D culture. In contrast to PEG, PAOx can be copolymerized to introduce a range of functional side-chains including vinyl groups suitable for thiol-ene photochemistry [13-15]. Conjugating cell adhesion motifs, such as arginine-glycine-aspartic acid (RGD), allows PAOx structures to

Correspondence to: Danica K. Hickey, Institute of Health & Biomedical Innovation, Queensland University of Technology, Australia, Tel: +61 7 3138 6239; E-mail: danica.hickey@qut.edu.au

Tim R. Dargaville, Institute of Health and Biomedical Innovation, Queensland University of Technology, Australia, Tel: +61 7 3138 2451; E-mail: t.dargaville@qut.edu.au

Key words: *3-dimensional tissue culture, poly (2-oxazoline) polymer scaffolds, primary human tissue culture*

Received: January 03, 2017; **Accepted:** January 19, 2017; **Published:** January 23, 2017

provide selective cellular interactions. Farrugia *et al.* has shown that polymer conjugation with RGD actively increases primary fibroblast cells adhesion to PAOx structures [16]. Further, the hydration of PAOx is similar or greater than PEG, giving it a "water-like" structure which reduces protein interactions and limits undesired biological interactions [17]. Current literature suggests a wide variety of potential biomedical uses of PAOx as a synthetic biomaterial [16, 18, 19]. While research and interest into PAOx has increased greatly in recent years, little of this research has focused on PAOx based hydrogel structures as 3D tissue culture scaffolds [13].

To date cross-linked hydrogels used for 3D cell culture require the encapsulation of live cells during UV curing [20]. Although this method has shown to support growing cells [20], UV induced DNA damage limits this technique's use for wider 3D tissue culture scaffold applications [21].

Our work aims to translate cross-linked PAOx hydrogels into a synthetic cell-compatible scaffold for bio-inert 3D tissue culture. In this study, we develop a novel encapsulation method for cell distribution into PAOx that negates the potential for UV DNA damage of cells. Through the controlled addition of RGD integrin binding peptide within PAOx the addition and growth of both immortalized and primary cell lines, each differing growth characteristics, can be sustained.

Materials and methods

PAOx hydrogel synthesis

The hydrogel pre-polymer, poly(2-methyl-2-oxazoline-*co*-2-undecenyl-2-oxazoline), was synthesized with a ratio of 2-methyl-2-oxazoline to 2-undecenyl-2-oxazoline of 190:10 ($PMeOx_{190}$-$DecenOx_{10}$) according to a previous method [15]. Stock solutions of the hydrogel reagents (all in double distilled water (ddH_2O)) were prepared as following: 13.5% w/v solution of $PMeOx_{190}$-$DecenOx_{10}$, 10% w/v dithiothreitol (DTT) (Sigma-Aldrich, Australia), and 2% w/v Irgacure 2959 (I2959) (BASF, Australia). To make the hydrogels a solution combining 151 µL of $PMeox_{190}$-$Decenox_{10}$, 9.1 µL of I2959, 7.6 µL of DTT stocks and 13.3 µL of ddH_2O. Cured hydrogel discs were prepared by pipetting 38 µL of hydrogel precursor solution as a single beaded drop between slides coated in Sigmacote (Sigma-Aldrich, Australia) spaced 1 mm apart vertically. A fiber optic cable was placed 3 cm from the slides and the hydrogel cured under 365 nm light for 540 seconds (Omnicure S1000 UV lamp). Hydrogels were washed with and kept stored in ddH_2O at 4°C.

RGD-conjugated PAOx hydrogels

Hydrogel precursor mix was prepared as above, with the addition of 1% w/v cysteine–arginine–glycine–aspartic acid–serine–glycine aqueous solution (C**RGD**SG; Mimotopes, Melbourne). The mixture was irradiated using 365 nm UV light for 120 seconds (3 cm) to conjugate the RGD containing peptide to the polymer. Then 7.6 µL of DTT stock was added and 50 µL hydrogels were fully cured between slides as described above.

Freeze-drying

Hydrogels were frozen at -20°C, -80°C, or -196°C after excess water was aspirated from the samples. Hydrogels frozen to -196°C were removed from water and snap frozen in liquid nitrogen immediately prior to freeze-drying. Frozen hydrogels were freeze-dried overnight in open culture plate.

Scanning electron microscopy

Whole freeze-dried samples were cut open and oriented onto SEM pin stubs using stick on conductive carbon tabs. Samples were sputtered with a 10 nm thick coating of gold (Leica EM SCD005) and placed into the microscope (Quanta 200 scanning electron microscopy) for imaging.

Cell lines and primary cell culture

McCoy (mouse fibroblast, ATCC CRL-1696) and HFF (human foreskin fibroblast, ATCC SCRC-1041) cell lines were cultured in Dulbecco's modified eagle medium (DMEM) (Gibco, Thermo Fisher scientific, Australia) containing 1% v/v PenStrep (Gibco) (94 units/mL Penicillin, 94 µg/mL Streptomycin) and 5% v/v fetal calf serum (FCS) (Gibco). Primary fallopian tube stromal cells were provided for this project by the Queensland Fertility Group (QUT human ethics #1400000421). Fallopian tube stroma was isolated from whole tissue as previously described [22]. Briefly, tissues were rinsed with Hank's Balanced Salt Solution (HBSS) and minced under sterile conditions into 1–2-mm fragments and digested using an enzyme mixture containing 0.05% collagenase type IV (Sigma Aldrich, St Louis, MO) and 0.057kU/ul DNase (Sigma) for 1 h at 37°C. After digestion, cells were dispersed through a 250 µm mesh screen (Millipore) and filtered through a 20 µm mesh screen (Small Parts) to separate epithelial cells from stromal cells. Stromal cells were grown in a 50:50 v/v DMEM/ F12 medium (Gibco), containing 10% v/v FCS and 1% v/v Penicillin/Streptomycin.

Rehydration and seeding of hydrogel matrices

Lyophilized PAOx hydrogels we placed in 96-well plates rehydrated 200 µL of FCS free DMEM containing 1% v/v PenStrep. When hydrogels were fully hydrated, excess media was removed and scaffolds seeded with cells suspended in FCS free DMEM at concentrations of 1.5×10^5, 3.0×10^5, and 4.5×10^5 cells per hydrogel dependent on the experiment. Hydrogels were incubated with cells at 37°C in 5% CO_2 overnight, media was replaced with 200 µL of a 50:50 F12 media and DMEM containing 10% v/v FCS and 1% v/v Pen/Strep for growth for 72 hours at 37°C in 5% CO_2.

Cell staining

After 72h incubation, the media was removed and PAOx washed twice in PBS for 5 minutes each. Cells were fixed in 100 µL of 4% paraformaldehyde (PFA) for 20 min before being washed twice in PBS and stored at 4°C for staining. For staining gel was washed 2 times with PBS to and stained with 50 µL of stain solution for 30 min at room temperature under foil. Stain was removed and wells washed with 100 µL of DMEM containing 5% FCS and 2 washes of PBS before fixing in 4% PFA. Following PFA fixation the samples were stained with 50 µL of Eosin Y (2′,4′,5′,7′-tetrabromofluorescein) (Merck, Australia) to visualize the polymer. Scaffolds were stained for 2 min at room temperature before eosin was removed and each scaffold washed twice with 80% ethanol, and twice with PBS. For cell cytoskeleton and nuclear staining**,** 0.1% Triton-X (Merck) was added to permeablize cells for 20 min at room temperature. Triton-X solution was removed and 50 µL of stain solution containing 1: 40,000 DAPI (Thermo Fisher scientific), for nuclear material, and 1:40 Phalloidin 594 (Thermo Fisher scientific), for cytoskeleton, added for 20 min. Stain solutions were removed and scaffolds washed twice in PBS and kept refrigerated under PBS in the dark until microscopy.

Confocal microscopy

Stained PAOx scaffold stroma samples were removed from wells by separating the vertical edges with a small metal spatula. Orientation was maintained during sample extraction and samples were kept hydrated under PBS. PAOx scaffold stromal samples were placed in an inverted orientation onto a coverslip and examined under a Zeiss 780-NLO confocal microscope (Zeiss, Germany). Samples were excited with 405 nm, 514 nm, and 594 nm lasers. Z-stack images were generated examining up to 700 μm of the structure or until fluorescence could not be detected.

Data analysis and statistics

Quantification data from images collected from SEM and confocal microscopy was measured using ImageJ software package (National Institutes of Health, USA). Based on the known scale included in the images the area select tool within the software and a graphics tablet (Wacom) was used to measure the 2D open area of pores on images at 60 μm intervals within the sample z-stack**.** As this was an optimization of method and characterization of gels statistical analysis was only appropriate for comparing the effect with and without RGD on attachment and penetration. Unpaired t-test analysis was performed on data using Prism statistical package (Graphpad Prism 7, USA).

Results

Synthesis of PAOx hydrogels

PAOx hydrogels were prepared from a copolymer of 2-methyl-2-oxazoline and undecenyl-2-oxazoline synthesized by cationic ring opening polymerization according to a previous report (Figure 1) [15]. This method yields a low polydispersity (1.44) functional polymer in a single step [15]. Subsequent hydrogelation of the polymer was achieved using 365 nm light in the presence of the dithiol, DTT, and photoinitiator to yield discs with 5 mm diameter.

Generation of porous structures within PAOx hydrogels

When the McCoy B mouse fibroblasts were top-seeded onto non-porous PAOx gels in culture they were unable to penetrate into the gel and instead remained affixed to the top surface (data not shown). It was therefore hypothesized that if pores with suitable size and interconnectivity were introduced the hydrogels could be top-seeded but lead to the cells distributed throughout the gel. To do this firstly PAOx was frozen to induce ice crystals then dehydrated via freeze-drying to remove water to produce pores in solid PAOx structure. Here, pore formation using three freezing temperatures (-20°C, -80°C, and -196°C) prior to freeze-drying were examined. Figure 2A shows scanning electron micrographs (SEM) cross section of hydrogel samples following -20°C -80°C, and -196°C freeze-dry methods. For each temperature pre-freeze dry treatment unique variations in pore formation were observed (Figure 2A panels i-iii). PAOx that underwent -20°C freeze-dry pre-treatment displayed an internal structure of varied pore sizes with large pores interspersed with very small pores. In contrast, -80°C freeze-dry pre-treatment displayed a more consistent internal structure of medium to small pores. PAOx gels that were snap frozen in liquid nitrogen at -196°C prior to freeze-drying displayed a very fine porous structure on the outside of the hydrogel with a solid internal core. Furthermore, -196°C freezing resulted in a small fragile disc after freeze dry process. As such the brittle -196°C freeze-dry pre-treatment PAOx was not used further in this study. The variations in the visual pore sizes when PAOx is frozen at different temperatures suggests that the variability of pores is potentially due to the specific ice crystal size formed at each temperature during freezing prior to freeze-drying as represented in schematic 2B.

We next examined the stability of pore structures during rehydration of freeze-dried PAOx. The diameters of freeze-dried gels were measured before and after rehydration and compared to rehydration potential (Figure 3A). Following rehydration in -20°C freeze-dried PAOx recovered on average to 98.8% of the starting 5 mm diameter, while the -80°C and -196°C freeze-dry pre-treatment groups recovered 72.5% and 64% of the original diameters, respectively. Representative frames from a time-lapse of a -20°C freeze-dried PAOx can be seen in figure 3B, rehydration from 3.5 mm to fully swollen 5-6 mm diameter gels retained gel consistency similarly to the original cured PAOx gel, however pores, seen as bubbles, can be clearly observed following rehydration. To visualize pores in rehydrated gels, a novel staining method using Eosin Y couples with fluorescent confocal microscopy was used. Figure 5C shows confocal cross transverse z stack section of rehydrated gels following pre-freeze dried treatment at -20°C, -80°C and -196°C (Figure 3C panels i-iii). Similarly, to the SEM of freeze-dried gels, upon rehydration differences in size variations was also observed between each temperature tested. Further these variations mimicked those observed prior to rehydration suggesting that pores formed through freeze crystallization prior to freeze-drying allows for the stable expansion during rehydration of the gel structure to for a porous scaffold.

Characterization of rehydrated porous PAOx scaffold

To determine the variation or pores throughout rehydrated PAOx the 2D pore areas of transverse fields of view at 60 μm, 120 μm, and

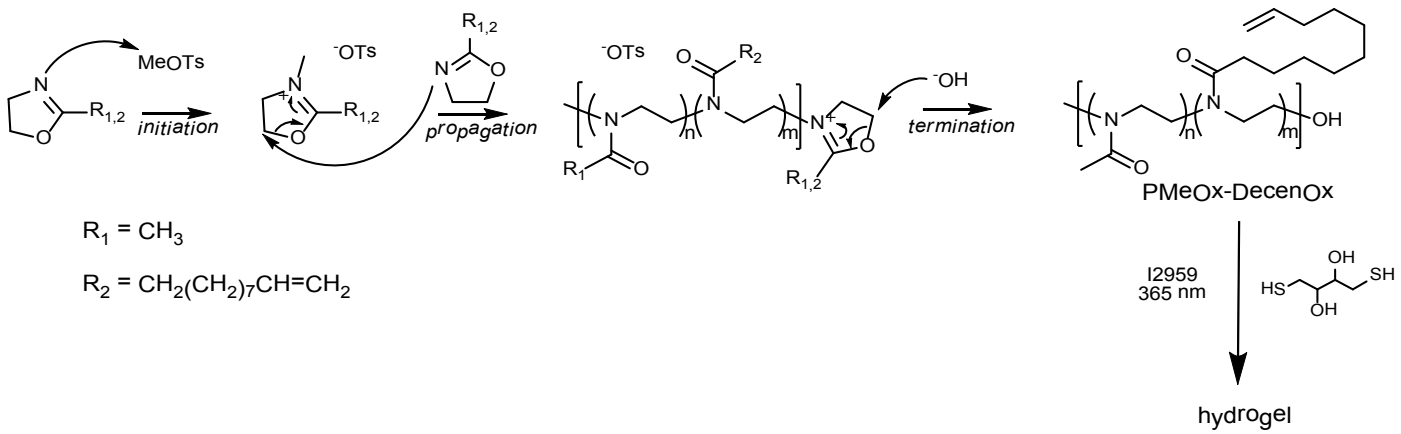

Figure 1. General reaction schematic of cationic ring opening polymerization of 2-oxazolines to form hydrogels in the presence of DTT, I2959 and 365 nm light.

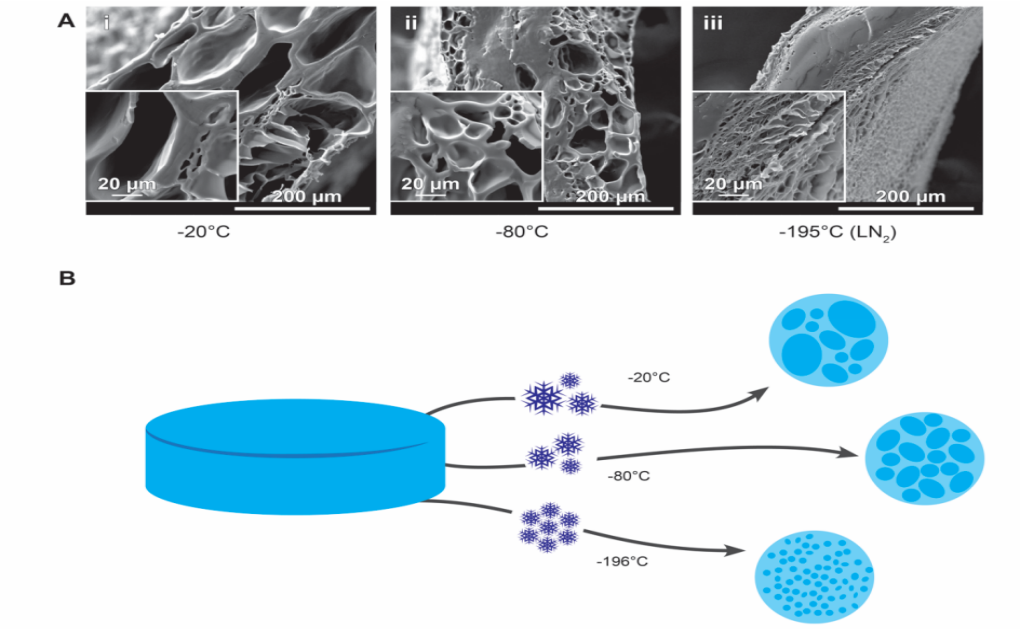

Figure 2. Freezing induced pores in the PAOx hydrogels. (A) Cured PMeOx-DecenOx PAOx hydrogels were frozen at -20°C (i), -80°C (ii) and 196°C (iii) before being lyophilized. Cross sections of the lyophilized hydrogel structures under scanning electron microscope (SEM) 600x, insert 2400x. (B) Proposed schematic outlining the different pre-treatments forming ice crystals inducing pore structures.

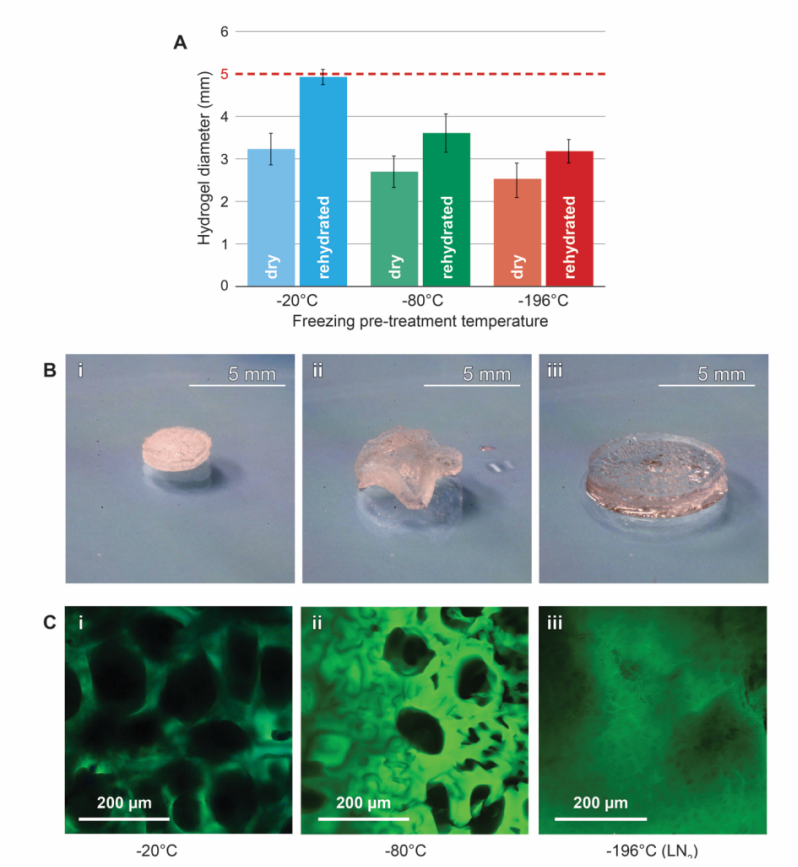

Figure 3. Rehydration of Freeze-dried PAOx hydrogels. (A) Average diameter of the -20°C (blue), -80°C (green) and -196°C (orange) samples before and after rehydration compared to starting 5mm cure PAOx (red dashed line). Data represents means ± SD of 8 gels). (B) frames from a time-lapse of a -20°C pre-treated hydrogel. Starting at a diameter of 3.5 mm in (i) an uneven swelling can be observed in (ii) resulting in a return to 100% of the original size and shape in (iii), scale bar = 5 mm. (C) swollen hydrogels from each of the pre-treatment freezing temperatures rehydrated and stained with eosin (green) when examined under confocal microscopy. Decreasing temperatures of pretreatments are displayed left to right, -20°C (i), -80°C (ii), and -196°C (iii) scale bars = 200 µm.

180 µm depth planes were measured using ImageJ as outlined in methods. Figure 3A shows examples of the pore sizes measured from a representative z-stack slice. By directly comparing mean and range of pore sizes at each depth a significant difference in pore area was obseved between 60 and 120 µm ($p<0.05$) and 60 and 180 µm ($p<0.01$) depths suggesting that porosity is not consistant throughour the entire gel for -20°C freeze-dry pre-treated PAOx (Figure 3B). In contrast, no significant difference in the pore varation was observed for -80°C freeze-dry pre-treated PAOx at all depths examined (Figure 3B) suggesting a more even pore size distrubution.

As shown in figure 3C, the frequency of each pore size throughout the measured PAOx hydrogels fall within a doubling area scale starting at 50 µm^2 and ending at to 12,400 µm^2. Compared to -80°C freeze-dried PAOx, -20°C freeze-dried PAOx results in high scaffold to scaffold variability across three individual gels examined (Figure 3C panels i and ii). Through measured individual cell types and cell cluster 2D area, the ideal pore area range, was determined to be between 200 µm^2 and 3,200 µm^2 to allow for cells to enter scaffold structures without passing straight through but large enough for growth and proliferation into cell clusters incorporating around 8 cells per pore. For -20°C freeze-dried PAOx only 39% of pores fall inside this theoretical zone, in contrast to -80°C freeze-dried PAOx in which 50% of pores fall within this range (Figure 3C panels i and ii).

Seeding of McCoy B fibroblast cell line into porous PAOx scaffolds

The generation of pores through freezing results in the variability of pore sizes and potential interconnectivity of pores allowing seeding and growth of cells throughout an interconnected scaffold. The McCoy B fibroblast cell line is highly adherent as such was used for initial seeding experiments of PAOx. Freeze-dried hydrogels were rehydrated overnight in FCS-free DMEM to ensure that any observed adhesion was not stimulated by growth factors present in FCS. Figure 5 shows that the incorporation and distribution of the McCoy B

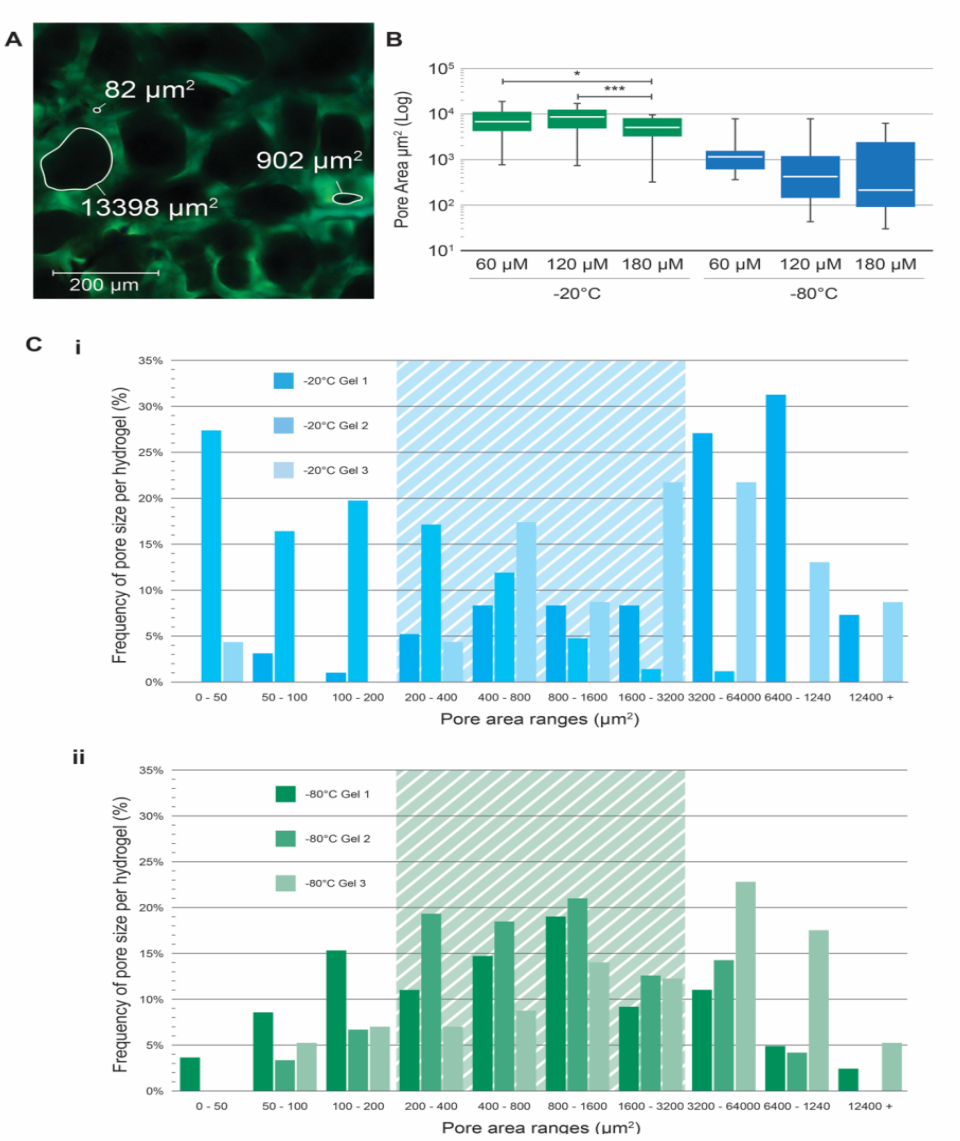

Figure 4. Variability of pore sizes in rehydrated PAOx. (A) Representative z-stack confocal image taken from -20°C pre-treated gel showing traced (white) and area calculated pore sizes (µm2) as labelled. scale bar = 200 µm. (B) Comparison of average pore sizes at 0 µm, 60 µm, and 120 µm slices into PAOx for -20°C and -80°C pre-treatments. Data represents means ± SD (n=3 gels). Comparisons between freezing methods were made by examining three planes from a confocal z-stack. **C** The frequency of pore sizes over the entire thickness of the observed area in -20°C (i) and -80°C (ii) pre-treated POAx. Shaded sections of the graphs depict the ideal pore size based on size of primary individual and small clusters of cells.

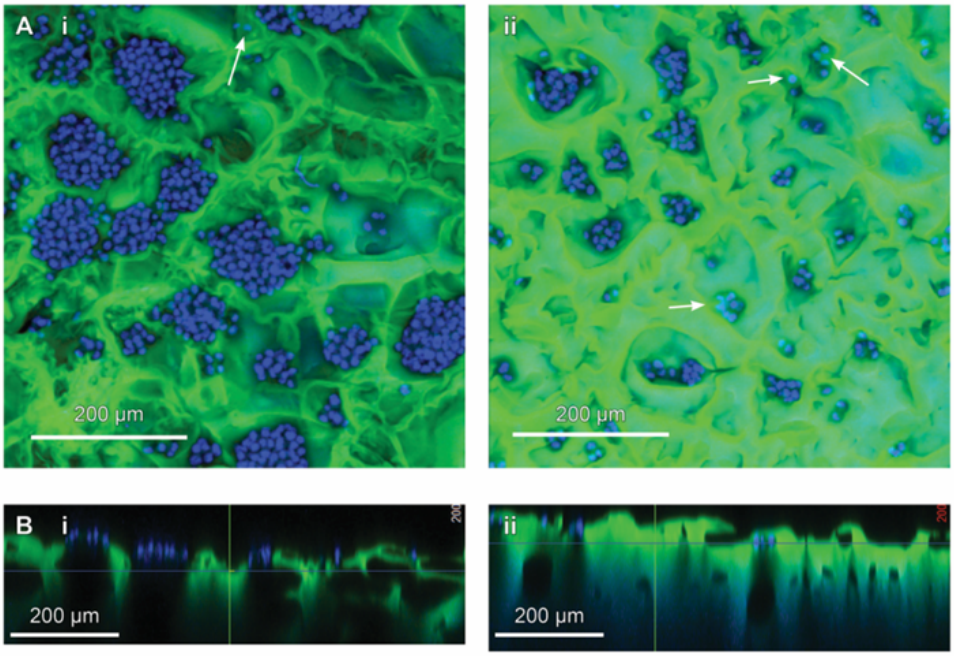

Figure 5. Pre-treated porous PAOx hydrogels as scaffolds for McCoy cell growth. (A) z-stack of PAOx scaffold stroma samples stained for nuclear material (DAPI, blue), and scaffold (eosin y, Green). Cells can be seen growing in clusters of varying sizes when seeded onto -20°C (i) and -80°C (ii) pre-treatment samples from top of the confocal z-stack (scale bars = 200 µm). Clusters larger in size and with a higher variability in cell population can be seen growing on the -20°C pre-treatment samples (i) when compared to smaller more regular clusters of cells observed growing in the -80°C pre-treatment samples (ii). Further, the semi translucent nuclei seen (arrows) are cells present below the surface of the scaffold. (B) Cross-section of the -20°C (i) and -80°C (ii) samples generated from the z-stack images which displays some of the underlying scaffold architecture

cells differs when seeded directly onto porous structures developed in -20°C and -80°C freeze-dried pre-treatment PAOx. Compressed confocal z-stacks of cells seeded onto hydrogels show that a -20°C freeze-dry pre-treatment results in the formation of large cell clusters that form predominately at the top of gels, whereas in -80°C freeze-dry pre-treatment smaller cell clusters were consistently distributed across the surface but also within gel as represented with arrows (5A panels i and ii). Within side view z-stacks, blue ghosting colour can be observed representing cells within the -80°C freeze-dry pre-treated gel structure but not -20°C freeze-dry pre-treated gels (5B panels i and ii). This suggests that for -20°C freeze-dry pre-treated gels the large variability of pores sizing, with large pores interspersed with small pores, impedes cell seeding into gel structures and promotes surface growth. In contrast, -80°C freeze-drying pre-treatment induce more uniformed size structures between 200 and 3000 µm readily promotes the introduction of cells into gels resulting is small but dispersed clusters throughout. As such -80°C freeze-drying pre-treatment were used for the generation of PAOx scaffolds for 3D tissue culture production.

Functional conjugation of high RGD concentrations alters cell penetration and morphology

Unlike cell lines, primary cell lines are less adherent and so a common strategy is to attach integrin binding peptides such as RGD. RGD has shown to affect both cell attachment and characteristic growth morphology. Figure 6A shows a schematic of RGD and conjugation of this functional group to the PAOx network. Here, using the highly adherent McCoy B cell line which we have observed to distribute throughout -80°C freeze-drying pre-treatment PAOx, we investigated the effect of RGD concentration on depth of cell penetration following apical seeding into PAOx. Figure 6B shows that the penetration of McCoy B cells into gels incorporated with 0% or 1% w/v did not have a significant effect on the incorporation of cells into the PAOx scaffold. In contrast a significant inhibition of cell penetration compared to no RGD control was observed with 2.5% ($p<0.05$), 5% ($p<0.01$) and 10% ($p<0.001$) w/v conjugated RGD. This suggests that at high concentration RGD cells readily adhere to at apical sites of PAOx and are not distributed into deeper gel layers. We further show that the normal spindle-like fibroblast morphology is observed with less than 1% RGD (Figure 6C, panels i and ii) while spindle morphology is inhibited resulting in more rounded compact cell morphology observed at higher RGD concentrations (2.5%, 5% and 10%) (Figure 6C, panels iii-v). This suggests that the multiple RGD adherence sites in in PAOx conjugated with >1% RGD inhibits both the penetration of cells into PAOx and the extension of normal fibroblast morphology.

Generation of PAOx scaffold in vitro 3D human stroma

Our primary goal is to develop a PAOx scaffold to support the growth of human primary *in vitro* 3D tissue culture. Here we compared the HFF1 human fibroblast cell line or primary human fallopian tube stromal cells for adherence to PAOx scaffolds with and without 1% conjugated RGD. Figure 7A is a compressed confocal z-stack showing cells present in PAOx scaffolds (indicated by white arrows). Preliminary staining with Zombie Aqua was performed to examine the viability of the cells within the structures; however little to no sign of cell death was seen. We expect dead cells would not remain adhered to PAOx. Interestingly, HFF1 cells grew as singular or small clusters with a rounded morphology in PAOx with and without 1% RGD (Figure 7 A, panels I and ii). In contrast, the morphology of primary human fallopian tube stromal cells differed with the addition of 1% RGD.

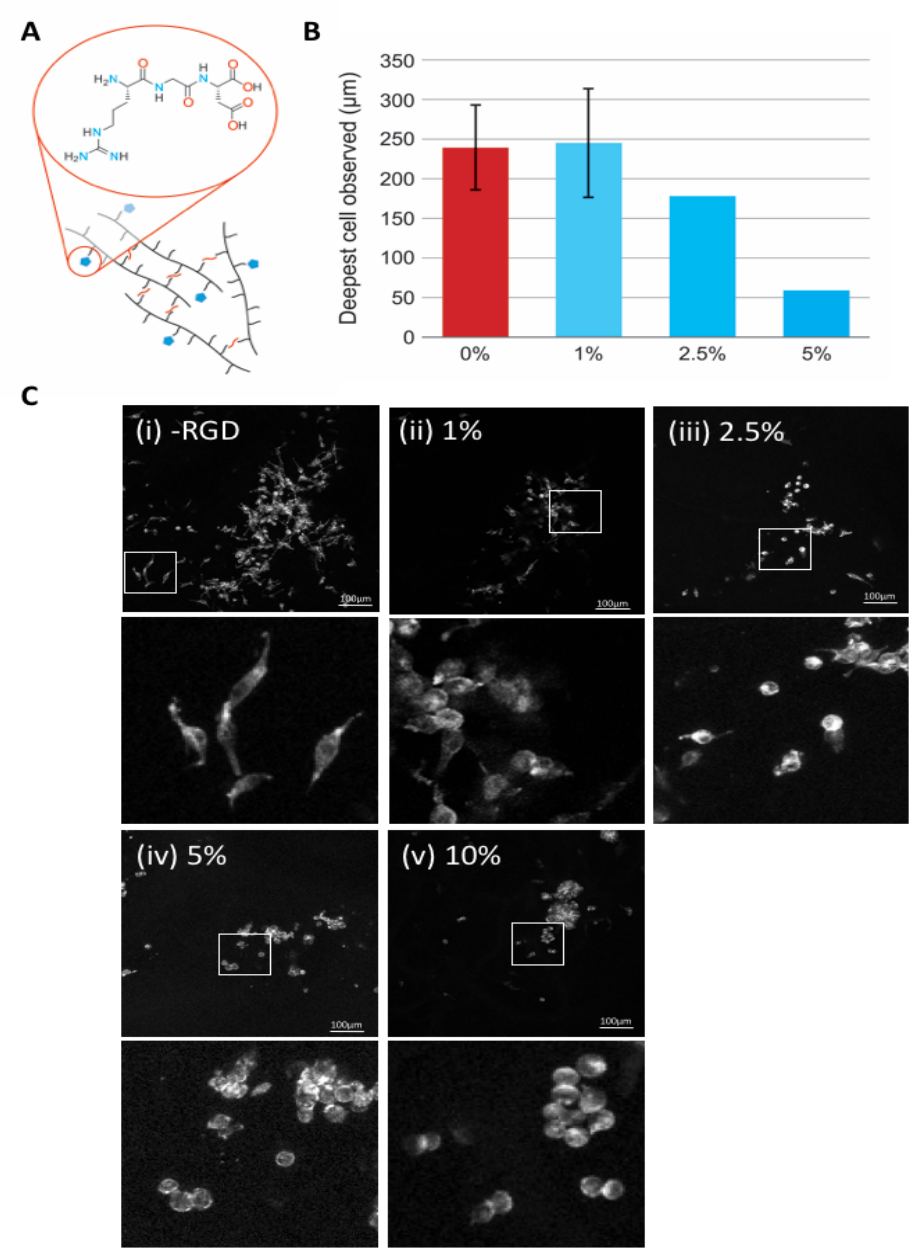

Figure 6. RGD concentration effects on cell adherence and morphology. (A) Schematic of the functionalization of -80°C pre-treated and rehydrated PAOx structures with RGD. (B) Mean penetration (µm) of McCoy B cells in PAOx containing 0%, 1%, 2.5%, 5% and 10% RGD w/v. data shows 4-8 confocal field depths. (C) Representative images of McCoy B cell growth in PAOx containing 0% (i), 1% (ii), 2.5% (iii), 5% and (iv) 10% RGD w/v with zoomed images for each RGD concentration below.

Figure 7B show cells growing beneath layers of PAOx scaffold as semi-translucent and examples of this are indicated with white arrows on panels I, ii and IV. To characterize the depth of the cell growth and penetration, the final depth of cells was measured on the confocal software. While no significant difference in the penetration of HFF1 cells was observed between PAOx with and without 1% RGD, for primary human fallopian tube stromal cells 1% RGD was essential for the adherence of cells within PAOx with a significant decrease ($p<0.05$) in cell penetration observed in PAOx without 1% RGD (Figure 7B). It is noted here that we observed fewer primary human fallopian tube stromal cells in no RGD PAOx suggesting no adherence and the small amount observed in the top layers of the PAOx may suggest physical pore entrapment rather than bound cells.

Discussion

A biologically inert *in vitro* 3D tissue culture system is required for studies to elucidate coordinated immunological mechanisms of human cells under controlled conditions. To date many systems utilized in research have interfering biological elements. This study investigated the use of PAOx to generate a synthetic scaffold for the incorporation of living cells for *in vitro* 3D tissue culture. This work optimized a specific temperature free-drying and rehydration technique to generate scaffolds with optimal pore size and density while minimizing scaffold to scaffold variability during rehydration. The characterization PAOx pores was accomplished through a novel Eosin Y staining method developed here allowing for the visualization of hydrogel

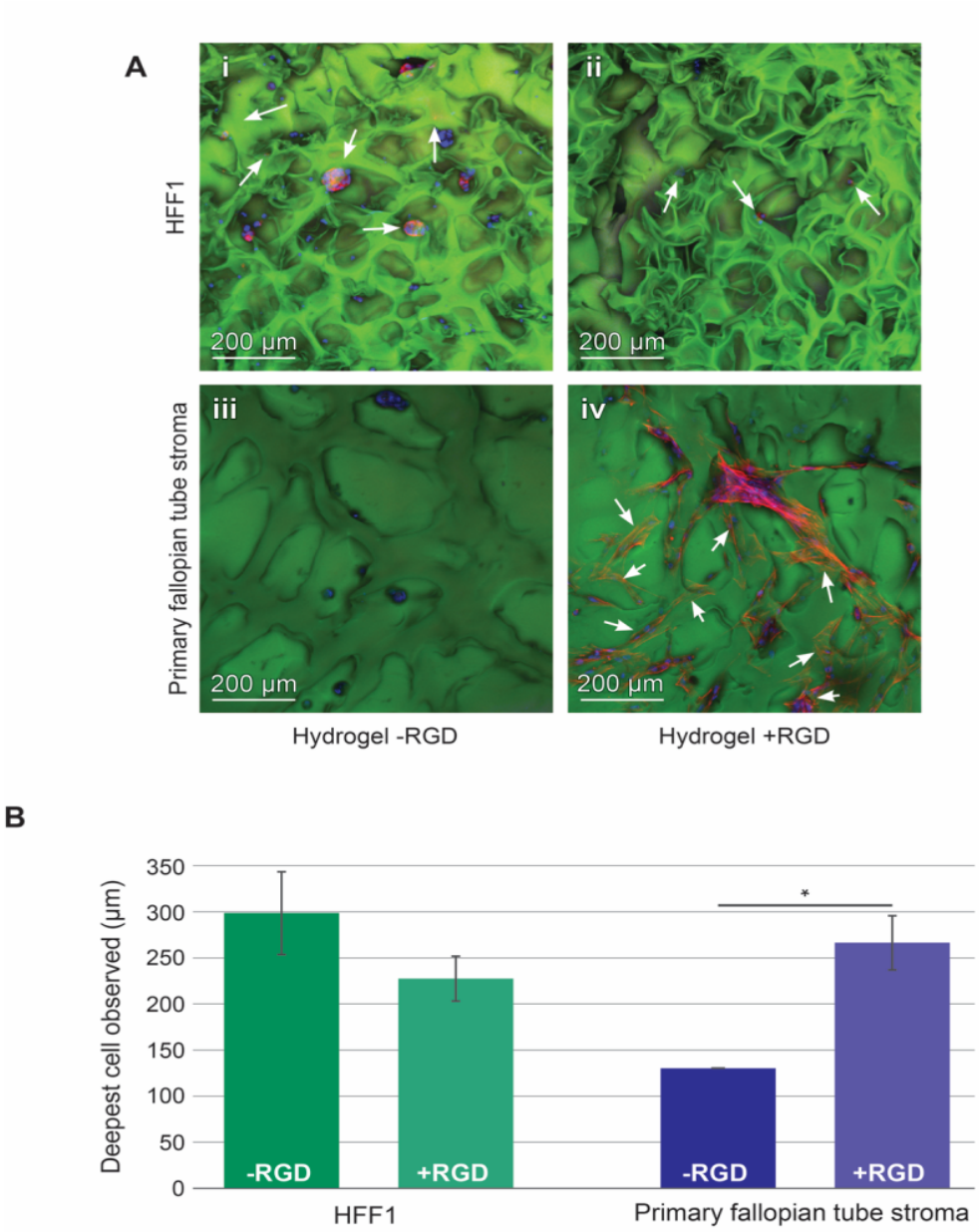

Figure 7. PAOx hydrogels as scaffolds for primary cell and cell line growth
(A) Representative images of -80°C pre-treated and rehydrated PAOx seeded with 3 x 10^5 HFF1 cells without RGD (i) or with 1% RGD (ii) and 1.5 x 10^5 primary human fallopian tube cells RGD (iii) or with 1% RGD (iv). PAOx scaffold stroma were stained to show nuclear material (DAPI, blue), scaffold (Eosin y, Green), and actin (Alexa Fluor 594, Red), samples were examined inverted under confocal microscopy (scale bars = 200 µm). (B) Cell depth into the hydrogel structures was measured and the deepest cells within the z-stack plotted. Depth of cells in hydrogels with and without RGD were compared via an unpaired t-test, * = $p < 0.01$, the data represent means ± SD (n=3 gels).

pore structures via confocal microscopy. Further, this study describes the functionalization of PAOx hydrogels with 1% RGD allows the adhesion of human primary reproductive tract stromal cells into a 3D matrix resembling the basic stromal tissue structure. The development of a human primary stroma shown here can form the basis of building 3D epithelial barrier tissue for *in vitro* studies.

We have previously demonstrated the ability to form PAOx hydrogels with a range of different swelling ratios using very simple synthetic methods [15]. The copolymer chosen for this study, $PMeOx_{190}$-$DecenOx_{10}$ cures rapidly (<30 sec) under aqueous conditions using 365 nm light and is amenable to modification with cysteine-containing peptides via thiol-ene photochemistry. The hydrogels are highly transparent to visible light when fully swollen making them useful for 3D cell culture.

A major limitation in the development and characterization of hydrogels and cell scaffolds is an inability to visualize the hydrogel substrate. Conventional techniques utilize SEM [24, 25] which requires samples to be dehydrated prior to coating with an electro conductive material such as gold. While this technique results in high resolution and high contrast images of samples providing valuable insights into structures, the ability to accurately characterize the structure of rehydrated hydrogels is not possible. In contrast to SEM, confocal

microscopy allows for the examination 3D scaffolds in a fully hydrated state [24, 26]. Current methods for the visualization of hydrogels in confocal microscopy requires the physical addition of bioactive sites such as heparin (to support the subsequent addition of fluorochromes) or to directly incorporate fluorescent dyes into the structure during synthesis [24, 26]. This approach can alter the chemical properties of the gels and possibly thereby induce non-specific protein adsorption and subsequent changes to cell behavior. Instead, we have developed a novel method for post synthesis hydrogel staining. In initial experiments the use of tissue histological techniques was examined for hydrogel visualization (data not shown). While the use of histology was unsuccessful for our hydrogels, as preparation of histological slides created undesirable porous artifacts, it was observed that PAOx could be stained with hematoxylin and eosin Y. The structure of PAOx and eosin prevents native binding; however, due to the slightly acidic composition of the eosin staining solution, that contains acetic acid, it is hypothesized that adsorption of the eosin occurs on the amide group of PAOx. Eosin is a derivative of fluorescein and can be excited at 514 nm [27, 28], and can therefore be combined with well-established techniques to determine a novel method for visualizing PAOx hydrogel scaffolds using fluorescent confocal microscopy.

For the development of *in vitro* 3D tissue culture systems, the incorporation of cells into the PAOx is required. Previous studies used UV encapsulation to distribute cells into hydrogel matrices [20]; however, UV exposure may produce DNA mutations that in turn may alter normal biological functions and responses although cells remain viable[21]. To avoid UV derived mutagenesis a post-synthesis cell distribution process through a porous scaffold structure is required. Many approaches to generating porous structures have been developed such as electrospinning, solvent exchange, and gas foaming [29]. For our future goal for the development of human 3D tissue culture the use of these methods are limited as they restrict which types of polymers that can be used, the lack of interconnected pores, or residual organic solvents which are toxic to mammalian cells. A method investigated here was the use of freeze-drying to generate ice crystals throughout hydrogels that when rehydrated result in an interconnected pore formation within solid hydrogels, that support cell delivery and growth. Ice crystal formation varies based on the contents of the water, the pressure within the system, and the rate and temperature of freezing [30-32]. Here it is shown that the size and shape of pores can be controlled through different freezing temperatures. For use in tissue culture, pores in scaffolds are required to be large enough to accommodate penetration of individual 600 μm^2 cells, sustaining small 3000 μm^2 cell clusters, and to act as ECM allowing for 3D adhesion. For this reason, snap freezing samples with liquid nitrogen cannot be used as it produces a porous structure too fine to allow cell penetration into the 3D structure. Here it is shown the range of pore sizes produced with pre-freezing at -20°C and -80°C temperatures are comparable. However, the regularity of these pores in a scaffold at an optimal size for cell cluster formation is consistent with -80°C pre-freezing temperatures, which display less scaffold to scaffold variation. Cryo-inducing pores in scaffolds also have an impact on the rehydrated macroscopic structure. Scaffolds typically rehydrate to 75% of the pre-processing dimensions with -80°C pre-freezing temperatures. However, the change in size when rehydrating scaffolds for specific purposes can be allowed and compensated for during production. Through freeze-drying and rehydration, the production of porous internal structures within hydrogels was achieved. While a good level of pore size and regularity was achieved here, more regularity in structure can be further optimized by controlling rate of freezing, induction of ice crystal nucleation sites, and altering the atmospheric pressures acting on the scaffolds during freezing. These pores not only facilitate the delivery and distribution of cells within a 3D scaffold but also support cell growth and the deposition of ECM by primary stromal cells.

For initial hydrogel tissue culture the mouse McCoy B fibroblast cell line was utilized for the highly adherent and non-fastidious nature of the cells. McCoy cells were shown to survive and proliferate when placed onto and in the scaffolds. The overall goal of the greater study is to develop 3D tissue culture scaffolds that imitate human tissue *in vivo*. Here human cell line (HFF1) and primary isolated human stromal tissue was assessed. Primary human cells are more fastidious, less adherent, and less proliferative than cell lines when cultured [33]; however, when grown in 3D with an ECM like environment primary cells have previously shown to grow for longer and in higher numbers[34]. The increased requirement for an ECM like structure explains the marked difference in cellular morphology and increased cell numbers when scaffolds were augmented with RGD. RGD is the cell-attachment domain found in fibronectin, an integral integrin in ECM [16, 23, 35]. The ability to selectively add specific functionality to scaffolds to enhance attachment or mimic the natural environment allows for direct experimental control over potential stimulating factors such as FCS, collagen, or Matrigel growth factors that are present in other 3D systems. These systems support *in vitro* growth but potentially mask or change biological response in many areas of research including those which examine hormone or drug interactions in biological systems. Due to the selectively included cell interactions displayed by PAOx scaffold stroma, this model has the potential to provide a low-noise model for selective hormonal investigations. These investigations will allow the elucidation of direct cellular and immunological impacts of hormones and growth factors present in human systems. Further, the low-noise nature of the model will allow clear investigations of cell-cell crosstalk between similar cells in culture and between cell types in physically connected co-culture models showing stromal and epithelial cells in a biologically relevant context. The biologically inert properties of PMeOx-DecenOx make it an ideal *in vitro* ECM substitute for tissue culture in 3D for models which demand high levels of control over cell stimulatory factors.

In this study, a novel freeze-dries and rehydration procedure was developed to induce a size controlled porous PAOx scaffold for use in 3D tissue culture. By employing staining commonly seen in histological analysis, the visualization and hence characterization of experimental outcomes are determined by a simple and inexpensive method in conjunction with routine confocal microscopy. Further, with the controlled addition of functional sidechains that mimic an ECM adhesion integrin, the attachment and growth of primary human stroma was achieved. Therefore, the utilization of the 3D PAOx scaffold model developed here for biological experimental designs involving human tissues that permit extended numbers of replicates can be achieved. The biological inert nature of PAOx provides a potential 3D structure that does not mask or stimulate critical biological results or processes that are regulated by small changes stimulated by hormones or drugs.

The novel PAOx scaffold developed here will provide a biologically inert stromal scaffold for the development of *in vitro* human epithelial barrier structures. PAOx supported *in vitro* tissue will provide for the study of the complex impact of extrinsic endocrine and immunological effects, as well as physical cell-cell cross talk on the biological functioning of tissues during infection. Further the tunability of PAOx

allows for greater control of biological additives, specifically tailoring PAOx to scientific need. Reliable bio-inert 3D cell scaffolds, compatible with primary human and other mammalian cells, will allow more accurate *in vitro* experimentation reflective of *in vivo* tissue.

References

1. Beagley KW, Gockel CM (2003) Regulation of innate and adaptive immunity by the female sex hormones oestradiol and progesterone. *FEMS Immunol Med Microbiol* 38: 13-22. [Crossref]
2. Abbott A (2003) Cell culture: biology's new dimension. *Nature* 424: 870-872. [Crossref]
3. Weaver VM, Petersen OW, Wang F, Larabell CA, Briand P, et al. 1997. Reversion of the malignant phenotype of human breast cells in three-dimensional culture and in vivo by integrin blocking antibodies. *J Cell Biol* 137: 231-245. [Crossref]
4. Bissell MJ, Hall HG, Parry G (1982) How does the extracellular matrix direct gene expression? *J Theor Biol* 99: 31-68. [Crossref]
5. Resau JH, Sakamoto K, Cottrell JR, Hudson EA, Meltzer SJ (1991) Explant organ culture: a review. *Cytotechnology* 7: 137-149. [Crossref]
6. Randall KJ, Turton J, Foster JR. 2011. Explant culture of gastrointestinal tissue: a review of methods and applications. *Cell Biol Toxicol* 27: 267–284. [Crossref]
7. Hughes CS, Postovit LM, Lajoie GA (2010) Matrigel: a complex protein mixture required for optimal growth of cell culture. *Proteomics* 10: 1886-1890. [Crossref]
8. Vukicevic S, Kleinman HK, Luyten FP, Roberts AB, Roche NS, et al. 1992. Identification of multiple active growth factors in basement membrane matrigel suggests caution in interpretation of cellular activity related to extracellular matrix components. *Exp Cell Res* 202: 1–8. [Crossref]
9. Tibbitt MW, Anseth KS (2009) Hydrogels as extracellular matrix mimics for 3D cell culture. *Biotechnol Bioeng* 103: 655-663. [Crossref]
10. Paxton JZ, Donnelly K, Keatch RP, Baar, K. 2009. Engineering the bone-ligament interface using polyethylene glycol diacrylate incorporated with hydroxyapatite. *Tissue Eng Part A* 15: 1201-1209. [Crossref]
11. Zalipsky S. 1995. Chemistry of polyethylene glycol conjugates with biologically active molecules. *Adv Drug Deliv Rev* 16: 157-182.
12. Lin CC, Raza A, Shih H. 2011. PEG hydrogels formed by thiol-ene photo-click chemistry and their effect on the formation and recovery of insulin-secreting cell spheroids. *Biomaterials* 32: 9685-9695. [Crossref]
13. Dargaville TR, Forster R, Farrugia BL, Kempe K, Voorhaar L, et al. (2012) Poly(2-oxazoline) hydrogel monoliths via thiol-ene coupling. *Macromol Rapid Commun* 33: 1695-1700. [Crossref]
14. Dargaville TR, Lava K, Verbraeken B, Hoogenboom R. 2016. Unexpected switching of the photogelation chemistry when cross-linking poly (2-oxazoline) copolymers. *Macromolecules* 49: 4774-4783.
15. Viegas TX1, Bentley MD, Harris JM, Fang Z, Yoon K, et al. (2011). Polyoxazoline: chemistry, properties, and applications in drug delivery. *Bioconjug Chem* 22: 976-986. [Crossref]
16. Farrugia BL, Kempe K, Schubert US, Hoogenboom R, Dargaville TR. 2013. Poly (2-oxazoline) hydrogels for controlled fibroblast attachment. *Biomacromolecules* 14: 2724-2732. [Crossref]
17. Konradi R1, Acikgoz C, Textor M (2012) Polyoxazolines for nonfouling surface coatings--a direct comparison to the gold standard PEG. *Macromol Rapid Commun* 33: 1663-1676. [Crossref]
18. Lück S, Schubel R, Rüb J, Hahn D, Mathieu E, et al. (2016) Tailored and biodegradable poly(2-oxazoline) microbeads as 3D matrices for stem cell culture in regenerative therapies. *Biomaterials* 79: 1-14. [Crossref]
19. Luxenhofer R, Schulz A, Roques C, Li S, Bronich TK, et al. (2010) Doubly amphiphilic poly(2-oxazoline)s as high-capacity delivery systems for hydrophobic drugs. *Biomaterials* 31: 4972-4979. [Crossref]
20. Dargaville TR, Hollier BG, Shokoohmand A, Hoogenboom R (2014). Poly (2-oxazoline) hydrogels as next generation three-dimensional cell supports. *Cell Adh Migr* 8: 88-93. [Crossref]
21. Tornaletti S, Pfeifer GP (1996) UV damage and repair mechanisms in mammalian cells. *Bioessays* 18: 221-228. [Crossref]
22. Rodriguez-Garcia M, Barr FD, Crist SG, Fahey JV, Wira CR (2014) Phenotype and susceptibility to HIV infection of CD4+ Th17 cells in the human female reproductive tract. *Mucosal Immunol* 7: 1375-1385. [Crossref]
23. Lava K, Verbraeken B, Hoogenboom R. 2015. Poly (2-oxazoline)s and click chemistry: a versatile toolbox toward multi-functional polymers. *Eur Polym J* 65: 98-111.
24. Borg DJ, Welzel PB, Grimmer M, Friedrichs J, Weigelt M, et al. 2016. Macroporous biohybrid cryogels for co-housing pancreatic islets with mesenchymal stromal cells. *Acta Biomater* 44: 178-187. [Crossref]
25. Luo Y, Kirker KR, Prestwich GD (2000) Cross-linked hyaluronic acid hydrogel films: new biomaterials for drug delivery. *J Control Release* 69: 169-184. [Crossref]
26. Lee SH, Moon JJ, Miller JS, West JL. 2007. Poly (ethylene glycol) hydrogels conjugated with a collagenase-sensitive fluorogenic substrate to visualize collagenase activity during three-dimensional cell migration. *Biomaterials* 28: 3163–3170. [Crossref]
27. Meallier P, Guittonneau S, Emmelin C, Konstantinova T. 1999. Photochemistry of fluorescein and eosin derivatives. *Dyes Pigm* 40: 95-98.
28. Acharya S, Rebery B. 2009. Fluorescence spectrometric study of eosin yellow dye–surfactant interactions. *Arabian J Chem* 2: 7-12.
29. Annabi N, Nichol JW, Zhong X, Ji C, Koshy S, et al. (2010). Controlling the porosity and microarchitecture of hydrogels for tissue engineering. *Tissue Eng Part B Rev* 16: 371-383. [Crossref]
30. Burton EF, Oliver WF. 1935. The crystal structure of ice at low temperatures. *Proc Roy Soc A: Math Phys Eng Sci* 153: 166–172.
31. Russell AB, Cheney PE, Wantling S.D. 1999. Influence of freezing conditions on ice crystallisation in ice cream. *J Food Eng* 39: 179–191.
32. Kang HW, Tabata Y, Ikada Y (1999) Fabrication of porous gelatin scaffolds for tissue engineering. *Biomaterials* 20: 1339-1344. [Crossref]
33. Smith C. 2005. Trouble in the hood: culturing difficult cell types. *Nat Meth* 2: 385–391.
34. Weber LM, Hayda KN, Anseth KS. 2008. Cell-matrix interactions improve beta-cell survival and insulin secretion in three-dimensional culture. *Tissue Eng Part A* 14: 1959-1968. [Crossref]
35. Krsko P, Libera M. 2005. Biointeractive hydrogels. *Mater Today* 8: 36-44.